J Chin Med Assoc

ORIGINAL ARTICLE

Combinatorial roles of mitochondria and cGMP/PKG pathway in the generation of neuronal free Zn^{2+} under the presence of nitric oxide

De-Ming Yang[a,b,c,*], Chien-Chang Huang[d], Yu-Fen Chang[e]

[a]Basic Research Division, Department of Medical Research, Microscopy Service Laboratory, Taipei Veterans General Hospital, Taipei, Taiwan, ROC; [b]Institute of Biophotonics, School of Medical Technology and Engineering, National Yang-Ming University, Taipei, Taiwan, ROC; [c]Biophotonics and Molecular Imaging Research Center (BMIRC), National Yang-Ming University, Taipei, Taiwan, ROC; [d]Core Facilities for Translational Medicines, National Biotechnology Research Park, Genomics Research Center, Academia Sinica, Taipei, Taiwan, ROC; [e]LumiSTAR Biotechnology, Inc., Taipei, Taiwan, ROC

Abstract

Background: Nitric oxide (NO), which possesses both protective and toxic properties, has been observed to have a complicated biphasic character within various types of tissues, including neuronal cells. NO was also found to cause the increase of another important signaling molecular Zn^{2+} (termed as NZR). The molecular mechanism of NZR has been extensively investigated, but the source of Zn^{2+} is present of a major candidate that is yet to be answered. The NO-protein kinase G (PKG) pathway, mitochondria, and metallothioneins (MTs), are all proposed to be the individual source of NZR. However, this hypothesis remains inconclusive. In this study, we examined the function of PKG signaling cascades, the mitochondria storage, and MT-1 during NZR of living PC12 cells.

Methods: We applied live-cell imaging in combination with pharmacological inhibitors and activators as well as *in vitro* Zn^{2+} assay to dissect the functions of the above candidates in NZR.

Results: Two mechanisms, namely, mitochondria as the only Zn^{2+} source and the opening of NO–PKG-dependent mitochondrial ATP-sensitive potassium channels (mK_{ATP}) as the key to releasing NO-induced increase in mitochondrial Zn^{2+}, were proven to be the two critical paths of NZR in neuronal-related cells.

Conclusion: This new finding provides a reasonable explanation to previously existing and contradictory conclusions regarding the function of mitochondria/mK_{ATP} and PKG signaling on the molecular mechanism of NZR.

Keywords: cGMP/PKG pathway; Mitochondrial K_{ATP} channels; Mitochondrial Zn^{2+}; NO; Zn^{2+}

1. INTRODUCTION

Nitric oxide (NO), a kind of unstable gas with a short half-life of 3–6 seconds, has been widely accepted as a common signaling molecule not only in cardiovascular and immune systems but also in neuronal-related cells.[1,2] The gas may have a protective function when the local NO content is controlled between 100 pM and 5 nM presumably through the contribution of neuronal NO synthase (NOS).[3] However, NO could be dangerously toxic at relatively high concentrations (μM), which are generally believed to be produced by inducible NOS (iNOS).[3] Such unique biphasic character of NO to neurons/brain has been previously observed.[2,4–6] The microenvironment of the neuronal system, which contains neurons and glia cells, is highly complex, with the emergence of NO occurring in at least three aspects: (1) the content scale of NO generated from various cell types; (2) the well-known NO/cGMP/protein kinase G (PKG) signaling pathway; and (3) the oxidative property of NO as reactive nitrogen species.

On the other hand, Zn^{2+} is one of the most important trace elements in virtually all living organisms. The metal ion is involved in multiple physiological reactions from the association and regulation of protein enzymatic functions and transcription factors to the expression of specific genes.[7,8] In addition, Zn^{2+} also participates in cell signaling.[9,10] In the neuronal system, Zn^{2+} can function as a neuroprotectant,[11] but low Zn^{2+} concentration or Zn^{2+} depletion can trigger the trend of apoptotic signaling in neurons confirms the free zinc ion's vital function.[12] On the contrary, Zn^{2+} was also found to be one of the critical factors to the progress of neurological disorders, such as cerebral brain ischemia/stroke, epilepsy, Parkinsonism, and Alzheimer's disease, among others.[12–14] Free-type Zn^{2+} ions co-exist with neurotransmitters in synaptic vesicles of several specific neurons, such as glutamatergic, γ-amino butyric acid (GABA)-ergic, and glycinergic neurons.[15,16] Therefore, a significant amount of Zn^{2+}, which could be highly toxic, will be transiently released upon

*Address correspondence: Dr. De-Ming Yang, Basic Research Division, Department of Medical Research, Microscopy Service Laboratory, Taipei Veterans General Hospital, Taipei 112, Taiwan, ROC. E-mail: dmyang@vghtpe.gov.tw (D.-M. Yang).

Conflicts of interest: The authors declare that they have no conflicts of interest related to the subject matter or materials discussed in this article.

Journal of Chinese Medical Association. (2020) 83: 357-366.

Received September 25, 2019; accepted November 17, 2019.

doi: 10.1097/JCMA.0000000000000280.

neuronal stimulation. Many upstream neurons have the ability to take up the released Zn^{2+} during neurotransmission and to transport Zn^{2+} back into the secretory vesicle again. In this recycling mode, Zn^{2+} toxicity could be lowered.[17]

NO can reportedly induce the release of Zn^{2+} (termed as NO-induced/dependent Zn^{2+} response, NZR) from metallothioneins (MTs) through the destruction of the S–Zn binding cluster with[18] or without[19] S-nitrosylation. Such hypothesis has been proven correct in specific cell types, including neurons.[20,21] Furthermore, NO/cGMP/PKG pathway, rather than MTs, activates the NZR in cardiomyocytes.[22] Compared with the NZR cascade in the cardiovascular system (PKG), that in the neuronal system seems quite different (MTs). However, there's no solid conclusion for what Zn^{2+} storage pool provides the main source of Zn^{2+} that gets released into cytosol (MTs or PKG, or others like mitochondria) by NO-induced signaling pathway. The major aim of this study is to investigate and clarify the molecular mechanism of NZR in neuronal cells, from NO to the following cGMP/PKG signaling cascade, and the role of mitochondria and the possible gate channels that release Zn^{2+}. In this study, we intensively dissected the functional roles of NO/cGMP/PKG signaling components and mitochondria in neuronal NZR.

2. METHODS

2.1. Reagents

The acetoxymethyl ester form (AM) of DAF, FluoZin-3, and RhodZin-3 were purchased from Life Technologies (Molecular Probes, Eugene, OR). All other reagents were purchased from the Sigma Chemical Company (St. Louis, MO) unless otherwise indicated.

2.2. Cell culture

Rat neuroendocrine pheochromocytoma PC12 cells were obtained from American Type Culture Collection (ATCC) and cultured as previous described.[23–25]

2.3. Live-cell imaging

Time-lapse ion imaging assay for the chemical-based fluorescent probes, ie, DAF to measure cytosolic NO, FluoZin-3 to measure cytosolic Zn^{2+}, and RhodZin-3 to measure mitochondrial Zn^{2+}, was carried out as previously described[24–26] with slight modifications. The cells were stained with specific indicators, eg, DAF (10 μM, 40 minutes at 37°C), FluoZin-3 (5 μM, 40 minutes at room temperature), or RhodZin-3 (5 μM, 30 minutes at 4°C), in a Ca^{2+}-free loading buffer and mounted in a recording chamber of an inverted microscope (IX-71, Olympus) with ×40 oil objectives (NA = 1.35, U/340) or a confocal microscope (LSM 5 Pascal, Zeiss, Germany) with ×63 (NA = 1.4) oil objectives. The cells stained with DAF, FluoZin-3, or RhodZin-3 were illuminated by a Xe lamp within a monochrometer (Polychrome V, T.I.L.L. Photonics, Germany) at 495/480 nm (for DAF /FluoZin-3) or at 550 nm (for RhodZin-3) or 543 nm laser under confocal imaging. The emission images of FluoZin-3/DAF or RhodZin-3 were obtained through the 505–520 nm band pass or 560 nm long pass filters, respectively. The images were collected using a high-speed cooled CCD camera (Orca AG, Hamamatsu Photonics, Japan) and recorded using SimplePCI 6.0 (Compix Inst.) or by a confocal microscope imaging system (LSM 5 Pascal, Zeiss, Germany). All live-cell imaging experiments were repeated thrice on different coverslips.

2.4. Reverse-transcription PCR (RT-PCR) assay

The PCR primers used to investigate the endogenous expression of MTs were designed as follows: Forward: CCGGAATTCCACCGTTGCTCCAGATTCAC; Reverse: CCCAAGCTTGGTGTACGGCAAGACTCTGA. The integrity of the total RNA, which was extracted from PC12 cells by using a cDNA synthesis kit (Thermo Sci.), was examined using 2% agarose gel electrophoresis, and RNA concentration was determined via UV light absorption at 260 nm. The RNA samples for RT-PCR were incubated for 30 minutes at 37°C with RNase-free DNase I and then for 10 minutes at 100°C to inactivate the DNase I. RT-PCR of the MTs from PC12 cells was performed with Finnzymes PCR reagents (Finnzymes OY, Finland) according to previously described procedures, including primer design and the general protocol for RNA extraction (Qiagen).[24–26]

2.5. Gene manipulations of MT-1

The MT-1 gene was cloned into two kinds of vectors: IRES for transfection within PC12 cells (MT-1-IRES-mOrange) and pASK-IBA15plus for transformation into *Escherichia coli* (pASK-IBA15plus_MT-1). Transfection of MT-1-IRES-mOrange into mammalian PC12 cells allowed for the observation of the live-cell NZR of overexpressed MT-1 (red arrows in the merged Fig. 3C) under the base of normal MT-1 expression (pure green stained in the merged Fig. 3C). For a large production of MT-1 protein to allow the subsequent *in vitro* Zn^{2+} assay, the bacteria were transformed with pASK-IBA15plus_MT-1 containing *Strep*-tag, as a previously described.[27,28]

2.6. *In vitro* Zn^{2+} assay

After the final step of protein purification prior to *in vitro* Zn^{2+} assay, MT-1 was placed on a 3-kD column. During a particular stage of the purification procedure, SDS-PAGE was performed to confirm the expression of MT-1 (Fig. 3E). A 3-kD column was first filled with 500 μL of purified MT-1 (MTs) proteins (1 μM), and then 500 μL of $ZnCl_2$ (10 μM) was added. The system was incubated for 60 minutes to allow the MT to fully bind the zinc ions. After washing for five times with Tris-HCl buffer (pH 7.6), the solution from the last washing was collected via centrifugation (14 000 rpm, 25 minutes, 20°C). The first portion was placed in the FluoZin-3 buffer mixed with an agent with or without NO donor (MT(–) is the empty column) flown through. The second portion was the solution collected via centrifugation after 60 minutes of incubation with NO donors (2 mM, 500 μL). The third part was the solution collected via centrifugation after 60 minutes of incubation in Tris-HCl (pH 2). A fluorescence spectrometer (Infinite M1000; TECAN, Switzerland) was used to assay the FluoZin-3 fluorescent signal.[27,28]

2.7. Immunocytochemistry and fluorescence microscopy

The MitoTracker Orange-stained PC12 cells were fixed by 3% paraformaldehyde for 20 minutes and permeabilized with 1% Triton X-100 for 15 minutes. The cells were incubated with MT-1 antibodies (1:100) overnight and then incubated with goat-anti mouse and rabbit (1:200) for 2 hours. The cells were imaged using a confocal laser scanning microscope (FluoView FV10i, Olympus, Japan) with ×60 (NA = 1.35, Olympus) objectives. To excite the secondary antibodies with green fluorescence and MitoTracker Orange, a 473-nm laser and a 559-nm laser were, respectively, used.

2.8. Statistical analysis

All experiments were conducted thrice with at least three different sets of cell samples. Data were gathered from different batches. The significance of changes at various conditions were validated based on p-values calculated using Student's t-test, with values set at $*p < 0.5$, $**p < 0.05$, $***p < 0.0001$.[26–28]

3. RESULTS

3.1. NZR exists in neuronal-related cells

First, we considered the NZR in living cells (live-cell NZR). The fluorescent indicators, DAF and FluoZin-3, were separately subjected to live-cell imaging to monitor cytosolic changes of NO (Fig. 1A,B) and Zn^{2+} (Fig. 1C,D), respectively, within the rat neuroendocrine pheochromocytoma PC12 cells. NO was supplied as the only external treatment onto intact living cells by three sources (NO donors), ie, sodium nitroprusside (SNP, triangle in Fig. 1A for NO; in Fig. 1B for Zn^{2+}), S-nitroso-N-acetylpenicillamine (SNAP, rectangle in Fig. 1A for NO; in Fig. 1B for Zn^{2+}), and spermine NONOate (circle in Fig. 1A for NO; in Fig. 1B for Zn^{2+}). This increase in cytosolic Zn^{2+} can be doubly confirmed as the real Zn^{2+} signal by adding the cell-permeable Zn^{2+} chelator, N,N,N′,N′-tetrakis-(2-pyridylmethyl) ethylenediamine (TPEN), by decreasing the fluorescent signal of FluoZin-3 (data not shown). A relatively strong correlation between the existence of NO and the elevated Zn^{2+} can be significantly observed (eg, comparison of the pattern in open and closed symbols in Fig. 1E,F). The data indicate that simply providing NO can induce the following increase in cytosolic Zn^{2+} within PC12 cells. According to the information acquired from live-cell imaging (Fig. 1A,B), spermine NONOate appears to be the most potent donor in producing significant amounts of NO. Spermine NONOate was therefore used as the major NO provider for subsequent live-cell NZR experiments.

3.2. Role of NO/cGMP/PKG cascade in the live-cell NZR

To determine the molecules that participate in live-cell NZR, we further examined the linkage of NZR between NO and Zn^{2+}. Given that the cGMP/PKG signaling pathway is the major route

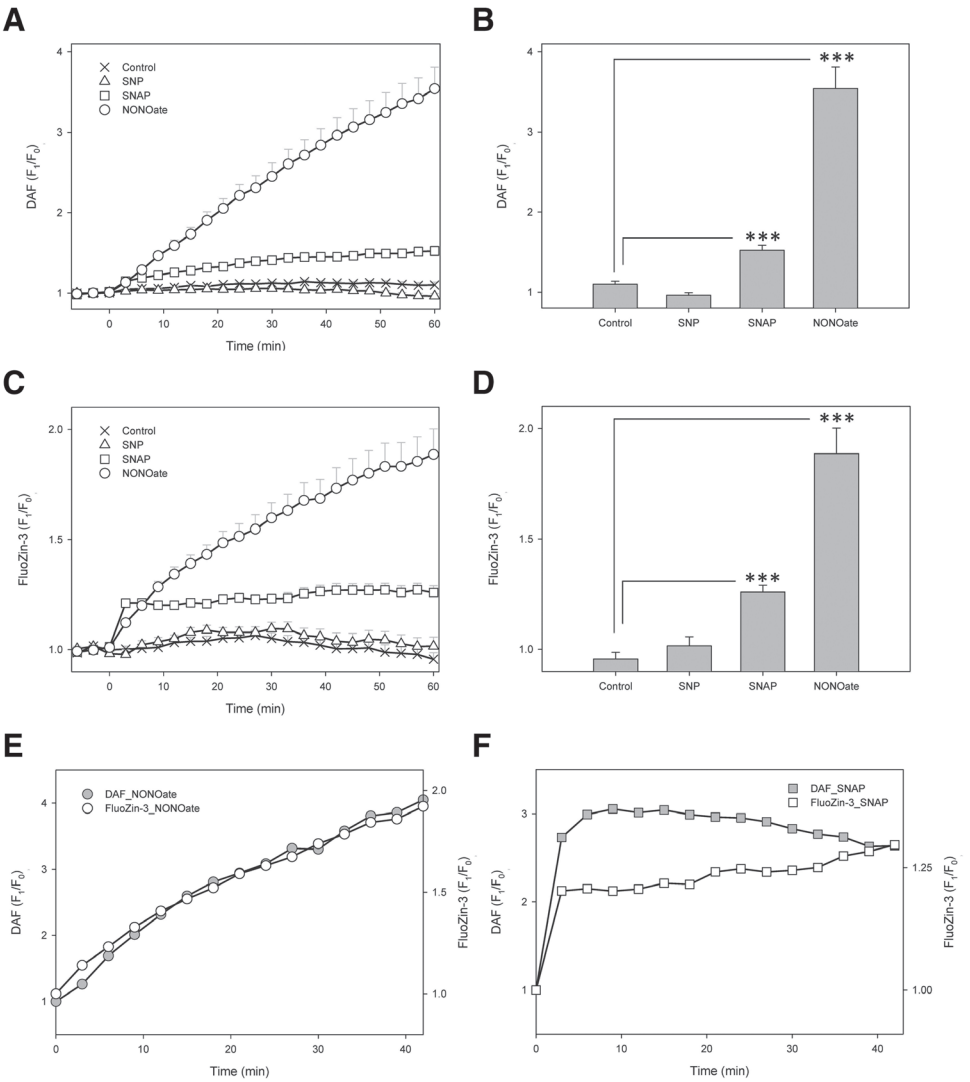

Fig. 1. The live-cell NO-induced Zn^{2+} response (NZR) can be observed within neuronal-related PC12 cells. Average curves within 60 min showing changes in the NO donor-induced increase in NO (A) or intracellular Zn^{2+} contents (C). **A:** Time-lapse recordings of intracellular NO generated from exogenous treatments of different NO donors, namely, SNP (triangle), SNAP (rectangle), or spermine NONOate (circle), compared with the control with physiological buffer (thin X). **B:** Bar graph showing the mean maximum value of relative NO signals (DAF, F_1/F_0) from each treatment in (A). **C:** Time-lapse recordings of intracellular Zn^{2+} under exogenous treatments of different NO donors, namely, SNP (triangle), SNAP (rectangle), or spermine NONOate (circle), compared with the control with physiological buffer (thin X). **D:** Bar graph showing the mean maximum value of relative Zn^{2+} signals (FluoZin-3, F_1/F_0) from each treatment in (C). **E** and **F:** Correlation between NO and Zn^{2+} can be further observed by comparing the plot of DAF and FluoZin-3 with that of spermine NONOate (E) or SNAP (F). Values are means ± SEM ***$p < 0.0001$, compared with the control.

by which NO exerts its physiological effects, we verified the function of PKG signaling molecules within live-cell NZR. By applying pharmacological tools, ie, inhibitors and/or activators of the signaling molecules, we dissected critical steps in NO/cGMP/PKG cascade during live-cell NZR (Fig. 2). The abolishment of spermine NONOate-induced NZR by the specific inhibitor of guanine cyclase (GC), ODQ (rectangle in Fig. 2A), and that of PKG KT5823 (triangle in Fig. 2A) confirmed the critical function of the NO/cGMP/PKG pathway in the link between NO and Zn^{2+} (Fig. 2B). The PKG inhibitor, KT5823, did not have any effect on the production of NO (Fig. 2C,D). The constitutive activator of cGMP, 8-Br-GMP, which can bypass the signal of NO, was further applied to test if the activity of GC and the following cGMP are enough to increase cytosolic zinc without NO (Fig. 2E,F). Contrary to predicted results, 8-Br-cGMP alone failed to initiate increased Zn^{2+} without the presence of spermine NONOate. The above data imply that the NO/cGMP/PKG pathway is relatively dominant but is inadequate in producing live-cell NZR. Therefore, particular targets of NO, such as MTs, are some of the candidate NZR sources.

3.3. Role of MT-1 in live-cell and *in vitro* NZR

Next, we wanted to investigate the function of MTs in live-cell NZR as well as *in vitro* NZR. The expressions of endogenous MTs within PC12 obtained via RT-PCR are shown in Fig. 3A,B. The data confirmed the existence of different MT isoforms expressed in PC12 cells, ie, MT-1, MT-2, and MT-3. To determine the exact function of the dominant form, MT-1,

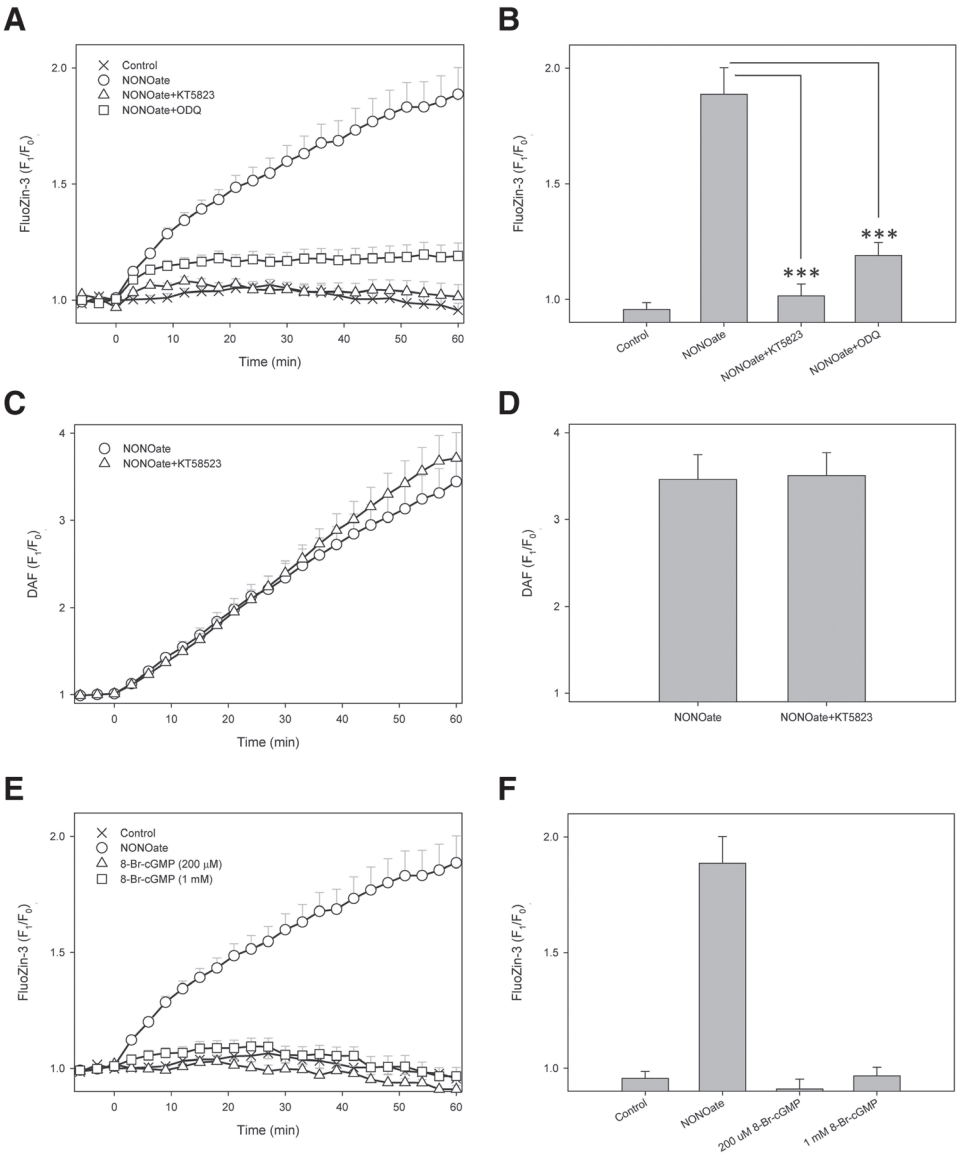

Fig. 2. NO/cGMP/PKG pathway is involved in live-cell NZR. Average curves within 60 min showing changes in NO donor-induced Zn^{2+} increase (A, E) and NO increase (C). **A:** Time-lapse recordings of intracellular Zn^{2+} under of spermine NONOate treatments without (circle) or with blockers, KT5823 (1 μM, triangle), or ODQ (5 μM, rectangle). **B:** Bar graph showing the mean maximum value of relative Zn^{2+} signals (FluoZin-3, F_1/F_0) from each treatment (in A). **C:** Time-lapse recordings of intracellular NO generated from spermine NONOate without (circle) or with the blocker KT5823 (triangle). **D:** Bar graph showing the mean maximum value of relative NO signals (DAF, F_1/F_0) from each treatment in (C). **E:** Time-lapse recordings of intracellular Zn^{2+} under 8-Br-cGMP treatments with different concentrations (200 μM in circle; 1 mM in triangle). **F:** Bar graph showing the mean maximum value of relative Zn^{2+} signals (FluoZin-3, F_1/F_0) from each treatment in (E). Values are means ± SEM ***$p < 0.0001$, compared with NONOate.

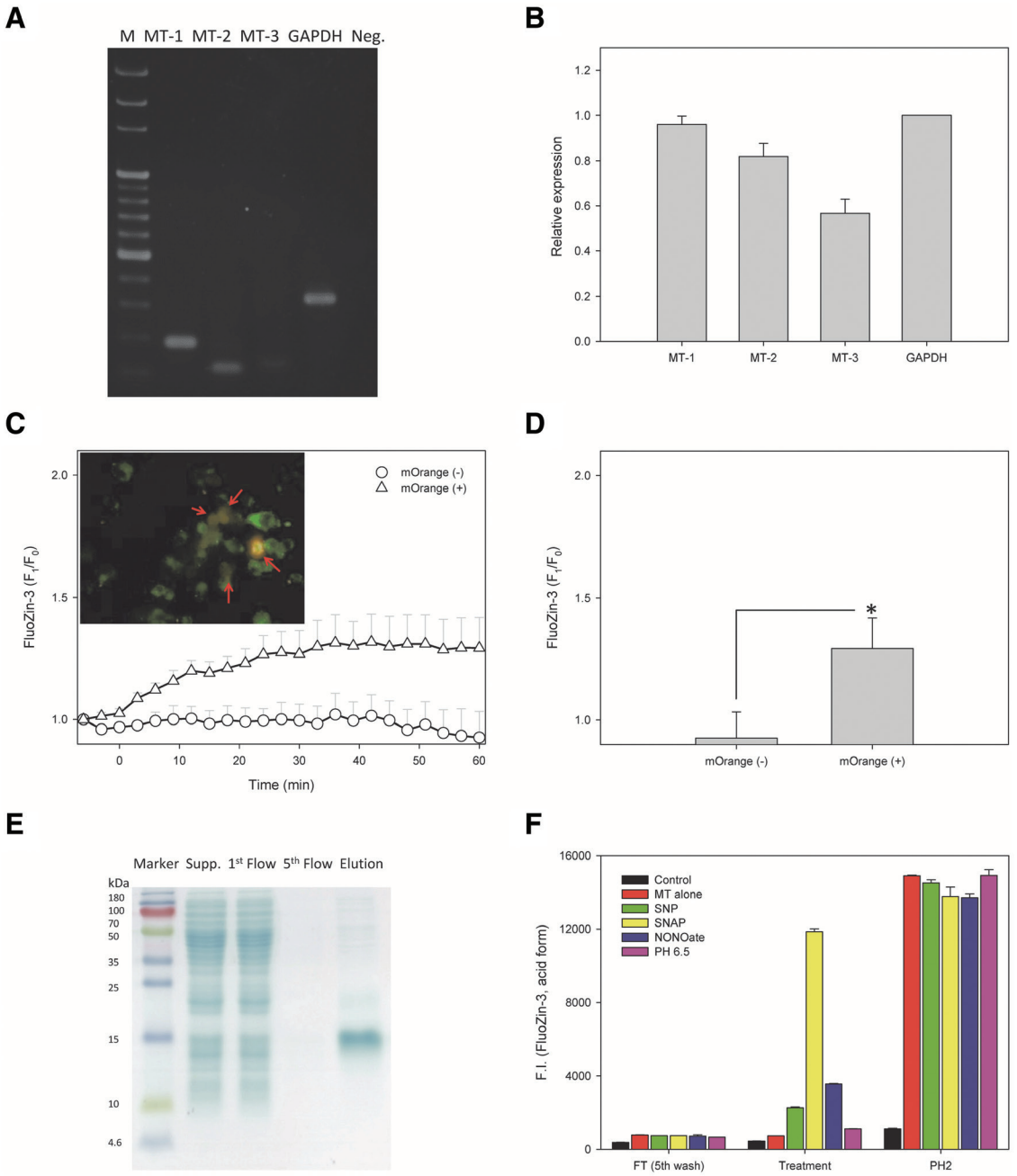

Fig. 3. Expressions and functions of MTs within neuronal-related PC12 cells for live-cell/*in vitro* NZR. **A,B:** Endogenous mRNA of MTs expressed in PC12 cells. **C:** Cloning and overexpressions of MT-1 protein within PC12 cells were identified using the selective red fluorescent protein mOrange (in left part of C, eg, arrows in right part in the merged image of C). Time-lapse recordings of intracellular Zn^{2+} under spermine NONOate treatment without (circle) or with overexpressed MT-1 (triangle). **D:** Bar graph showing the mean maximum value of relative Zn^{2+} signals (FluoZin-3, F_1/F_0) from each treatment in (D). **E, F:** *In vitro* Zn^{2+} assay. Values are means ± SEM *$p < 0.5$, compared with mOrange (–).

during NZR, we overexpressed the cloned MT-1 (together with mOrange fluorescent protein within the same IRES vector, see Material and Methods) into the PC12 cells. We compared the amount of live-cell NZR in MT-1 overexpressed cells (as indicated by arrows, with the red mOrange and green FluoZin-3 fluorescence, inset merged images in Fig. 3C) with that in the control cells (only with green fluorescence within the same tested coverslip, inset merged images in Fig. 3C). The live-cell NZR response of MT-1 overexpressed cells was significantly larger than that of the control cells (Fig. 3C,D).

To carefully confirm that the NO-dependent release of Zn^{2+} can solely originate from MTs, we purified MT-1 for the following *in vitro* Zn^{2+} assay (see Material and Methods). A large amount of the MT-1 protein was produced and purified from MT-1 transformed *E. coli* (Fig. 3E). The *in vitro* Zn^{2+} assay was exerted to demonstrate whether MT-1 alone is enough to release Zn^{2+} under the existence of NO (Fig. 3F). The fact that only the co-existence of MT-1 and NO can generate increased fluorescent signal of the Zn^{2+} indicator, FluoZin-3, suggests the function of MT-1 as a Zn^{2+} source of NZR *in vitro* (Fig. 3F). From the above

NZR experiments on MTs, we conclude that MTs perform a particular function in live-cell NZR as well as in NZR *in vitro*.

3.4. Mitochondrial K_{ATP} channels are the final step of live-cell NZR

Several PKG targets that lead to live-cell NZR have been proposed from previous studies, such as K_{ATP} channels on the mitochondrial membrane (mK_{ATP}), mitochondrial permeability transition pore (MPTP), cAMP response element-binding protein (CREB) in the nucleus, the Ca^{2+}-activated, large conductance K^+-channel on the cell surface, and ERK1/2-pGSK3β signaling molecules (evidence found in cardiomyocytes[29]). We further focused on the function of mK_{ATP} by means of the mK_{ATP} inhibitor, 5HD (triangle in Fig. 4A), and the MPTP inhibitor, cyclosporine A (CsA, rectangle in Fig. 4). The results show that mitochondria perform specific essential functions in live-cell NZR.

In addition, we also used the enhancer of mK_{ATP}, diazoxide, to confirm whether the gate opening of mK_{ATP} alone can generate NZR (Fig. 4C,D). Diazoxide was inadequate in generating a large increase in cytosolic Zn^{2+} as NONOate did, but still significantly (Fig. 4D) and is considerably similar to the above result in 8-Br-cGMP (Fig. 2E,F). mK_{ATP} appears to be the only gate that could allow the release of Zn^{2+} from mitochondria, although limited information exists on whether free Zn^{2+} can be generated within mitochondria. We predict that some unknown component(s) connects NO and bypasses the cGMP/PKG cascade to generate Zn^{2+} release from mitochondria during the generation of NZR. To prove this hypothesis, we treated cells with spermine NONOate under the presence of PKG inhibitor (KT5823) without or with the mK_{ATP} opener, diazoxide (Fig. 4E). Live-cell NZR still occurred under PKG blocking and the mK_{ATP} opener implies two new facts found in this study: (1)

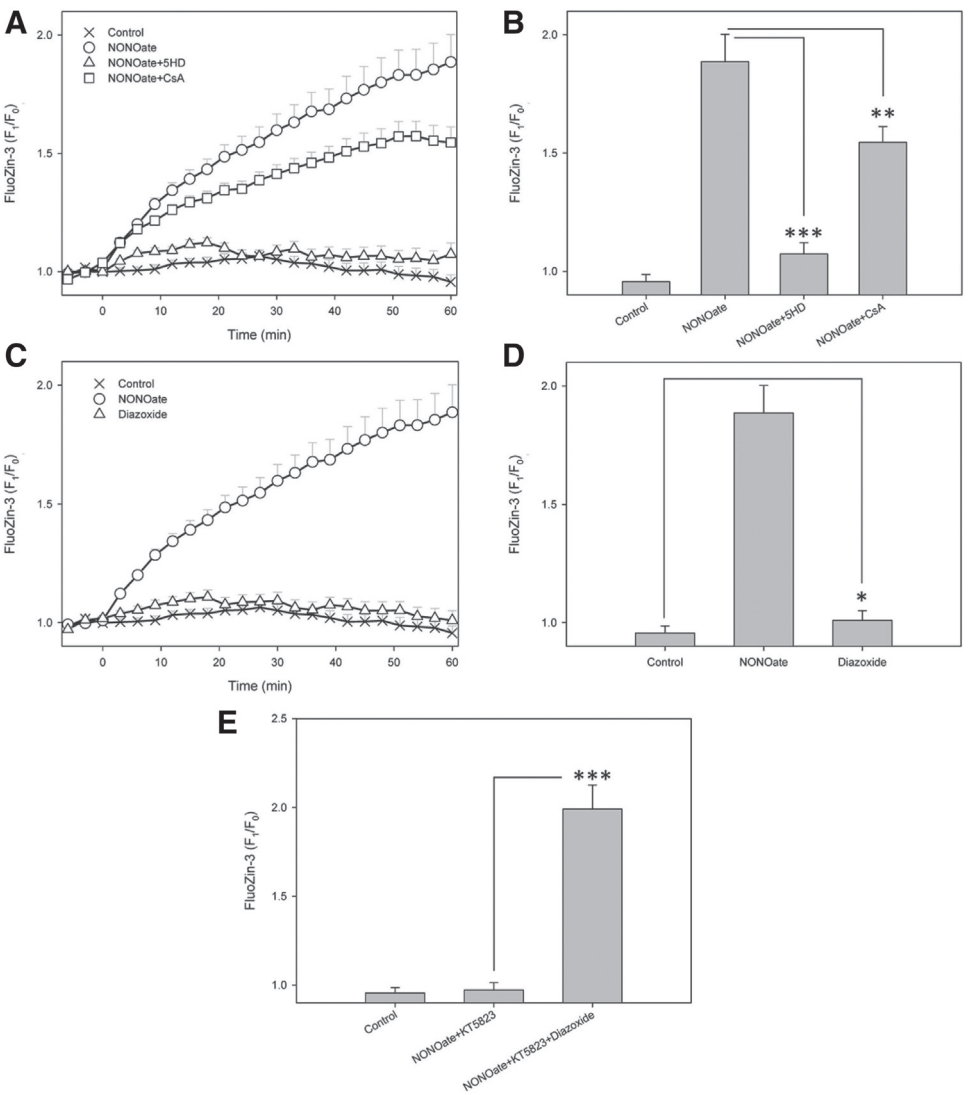

Fig. 4. The importance of mitochondria during live-cell NZR. Average curves within 60 min showing changes in NO donor-induced Zn^{2+} increase (A, C). **A:** Time-lapse recordings of intracellular Zn^{2+} under spermine NONOate treatments without (circle) or with mK_{ATP} blocker, 5-HD (500 μM, triangle), MPTP blocker, CsA (10 μM, rectangle). **B:** Bar graph showing the mean maximum value of relative Zn^{2+} signals (FluoZin-3, F_1/F_0) from each treatment in (A). **C:** Time-lapse recordings of intracellular Zn^{2+} under the treatments of the mK_{ATP} opener, diazoxide (500 μM, triangle). **D:** Bar graph showing the mean maximum value of relative Zn^{2+} signals (FluoZin-3, F_1/F_0) from each treatment (in C). **E:** Bar graph showing the mean maximum value of relative Zn^{2+} signals (FluoZin-3, F_1/F_0) in the presence of spermine NONOate without any blockers, with KT5823, or with KT5823 and diazoxide. Values are means ± SEM $^*p < 0.5$, $^{**}p < 0.05$, $^{***}p < 0.0001$, compared with NONOate (B) or the control (D) or NONOate + KT5823 (E).

mitochondria, as a unique Zn^{2+} pool, must be the source of NZR (the interaction of NO with the Zn^{2+} binding protein (ZnBPs), MT, or others still remain to be further identified); and (2) mK_{ATP} could be the main gate that releases the increased free Zn^{2+} from within the mitochondria.

3.5. NO-dependent increase of mitochondrial Zn^{2+}

To prove that Zn^{2+} increases inside the mitochondria, we measured the dynamic changes of mitochondrial Zn^{2+} with RhodZin-3 (Fig. 5). The resting state of mitochondrial Zn^{2+} under the presence of a mK_{ATP} inhibitor (5HD) was monitored via live-cell imaging (Fig. 5A; triangle in Fig. 5B) and finally imaged via confocal microscopy (left part, 5HD in Fig. 5D). Following the presence of NO (NONOate) and the gate closing agent, 5HD, the increase of mitochondrial Zn^{2+} was significantly observed (circle in Fig. 5B; right part in Fig. 5D), which suggests that NO may generate the increase in mitochondrial Zn^{2+}.

3.6. MT-1 did not translocate to mitochondria during NZR

Given that MT-1 can release Zn^{2+} (Fig. 3) and that mitochondria constitutes the cell location in which Zn^{2+} increases and is released (Figs. 4 and 5) by NO, we logically propose that MT-1 could be the exact source of Zn^{2+} within the mitochondria (exists within or translocates). Finally, in this study, we tested the possible role of MT-1 during live-cell NZR within the mitochondria via immunofluorescence assay combined with mitochondrial staining (green channel for MT antibody and red channel with MitoTracker Orange in Fig. 6). No significant translocation of MT-1 can be observed before (control) and after NO donor treatment (NONOate, 2 mM). This data suggest that maybe

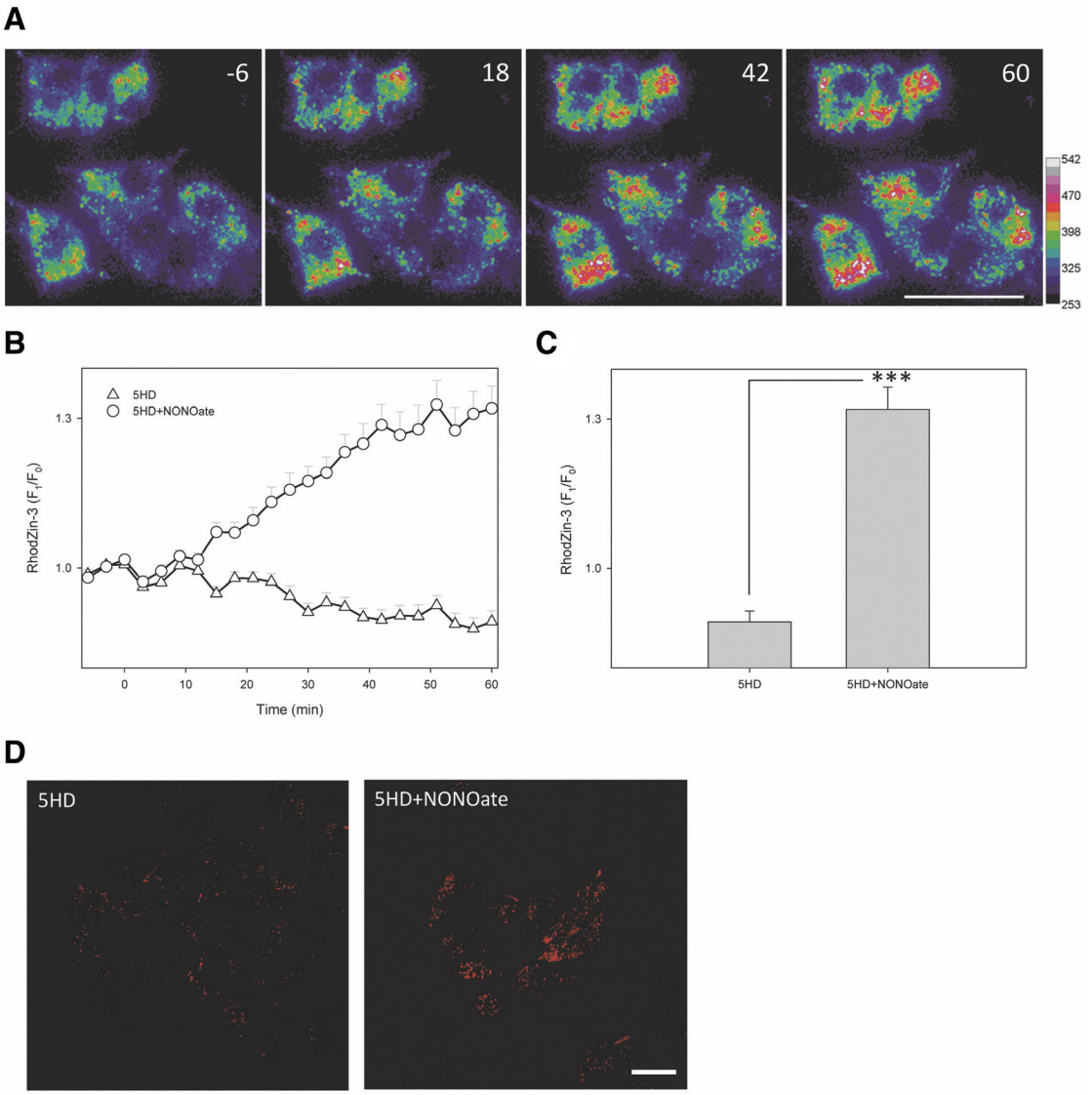

Fig. 5. Mitochondrial Zn^{2+} increase during live-cell NZR. **A:** Four representative time-lapse images of RhodZin-3 stained cells. The number shown on upper right side of each image represents the recording time as shown in (B). **B:** Time-lapse recordings of mitochondrial Zn^{2+} under spermine NONOate treatments without (circle) or with the mK_{ATP} blocker, 5HD (1 μM, triangle), or in the presence of 5HD alone (rectangle). **C:** Bar graph showing the mean maximum value of relative Zn^{2+} signals (RhodZin-3, F_1/F_0) from each treatment in (C). **D:** Representative images of RhodZin-3-stained PC12 cells under confocal microscopy with 5HD (left) or 5HD plus NONOate (right). These images were obtained immediately after live-cell imaging in (B). The color-coded scale bar in A ranges in fluorescent intensity from 253 to 542. The scale bars shown in right lower of A and D are 20 μm. Values are means ± SEM ***$p < 0.0001$, compared with 5HD alone in C.

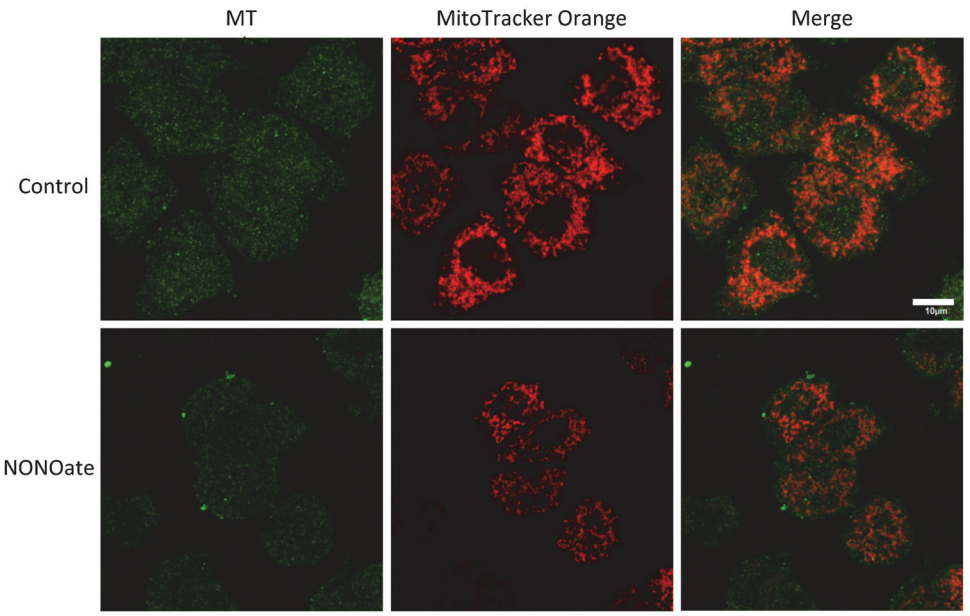

Fig. 6. Cytosolic localization of MT-1 within PC12 cells. Immunofluorescent images of MT-1 (left part in green) within PC12 cells under a confocal microscope indicate the localization of MT-1. To compare its specific localization, we stained the cells with MitoTracker Orange (middle part) at resting (upper part, Control) or in the presence of NO (2 mM of NO donor spermine NONOate, NONOate).

some ZnBPs and/or MT-1 together play the role as Zn^{2+} source within mitochondria during live-cell NZR.

4. DISCUSSION

From previous studies, we know that the biphasic property of NO is closely correlated with the amount of NO within local tissues. At normal physiological conditions, median NO levels can be generated via neurotransmission through both receptor-gated release of the chemical substance or electric-triggered activation. On the other hand, NO could be massively produced through iNOS (expressed in non-neuron cells such as astrocytes) at pathological conditions, such as cerebral ischemia/stroke, trauma, inflammation, and even the epilepsy. Zn^{2+} is one downstream result of NO, which has its own complicated mechanism both in physiological and pathological status. Clarifying the relationship and the molecular connections between NO signal and the subsequent increase in intracellular Zn^{2+} (NZR) is the major focus of this study.

The mechanism of live-cell NZR has been observed and studied in several types of cells.[22,29–32] In general, organelles and ZnBPs have been considered as candidate Zn^{2+} sources. Organelles such as mitochondria and/or nucleus have been both proposed.[33–35] MT-1, as a representative metalloprotein, was reported to be the major ZnBP that release Zn^{2+} under the presence of NO[30] or NO-induced acidification.[36–38]

From recent progress in metal ion bio-sensing, the contents of free Zn^{2+} within sub-cellular compartments are extremely low, eg, 0.1 pM in mitochondria and 1 pM in ER and Golgi compared with 200 pM in nucleus and 180 pM within cytosol.[39] The result that free zinc ions can be released from such sub-cellular compartments at a resting state seems impossible, but the linkage between the dominant function of the PKG pathway and the essential function of mK_{ATP} during live-cell NZR was found to be true in cardiomyocytes[22] and in neuronal cells (present study). Thus, mitochondria are unlikely to be the Zn^{2+} source unless a large amount of ZnBP-carried Zn^{2+} exists within the mitochondrial space (stimulated by NO). To date, available information about NO–PKG signaling stops at the mitochondria (mitochondrial K_{ATP} channels) and the source of Zn^{2+} (some unknown ZnBPs and/or MTs) still remains to be identified.

Regarding the effects of 8-Br-cGMP and diazoxide, our results in neuronal cells did not agree with previous findings (comparison of Fig. 2E,F with results of Jang et al., 2007[22]). In other words, 8-Br-cGMP or diazoxide alone can induce Zn^{2+} response within cardiomyocytes (but not neuronal cells) even without the existence of NO. Meanwhile, the conclusion that PKG is the only pathway to exert live-cell NZR cannot provide further information on the relationship between mitochondria (mK_{ATP}) and NZR. In our study, the finding stating that the PKG–mK_{ATP} route is insufficient to generate Zn^{2+} response in the absence of NO in neuronal cells (Fig. 2E,F) implies the existence of another path in addition to the PKG cascade. Therefore, we returned to the mitochondria and considered the possibility of a NO-dependent increase in mitochondrial Zn^{2+} at the closing state of mK_{ATP} channels (Fig. 5). We proposed that NO directly enters into mitochondria and reacts with ZnBPs, in which MTs may not be totally excluded, to increase free Zn^{2+} contents within the mitochondria. Several reports actually observed the phenomena of mitochondrial Zn^{2+} increase under the presence of NO[40,41] or pathological conditions like ischemia.[42,43] Therefore, we confirmed the mitochondria to be the NO-dependent Zn^{2+} pool. Following this confirmation, we further proposed that NO–cGMP/PKG-dependent opening of mK_{ATP} channels could logically be the main gate that allows the increase in mitochondrial free zinc ions (generated by NO) that enter into cytosol (Fig. 5). However, the exact molecular components of mK_{ATP} channels are still inconclusive.[44,45] Despite our limited ability to further explain the detailed mechanism of Zn^{2+} permeability by mK_{ATP}, we are the first to propose the new function of mK_{ATP} gating of Zn^{2+} from mitochondria to cytosol in an NO–PKG-dependent manner. The existence of an unknown mitochondrial channel protein that is directly or indirectly regulated by mK_{ATP} to release Zn^{2+} presents a compelling speculation.

On the other hand, ZnBPs that are widely expressed throughout the neuronal cells were observed to be the Zn^{2+} pool, specifically with changes in intracellular pH.[38] Notably, several reports also observed that cytosolic pH can be influenced by NO.,[36–38]

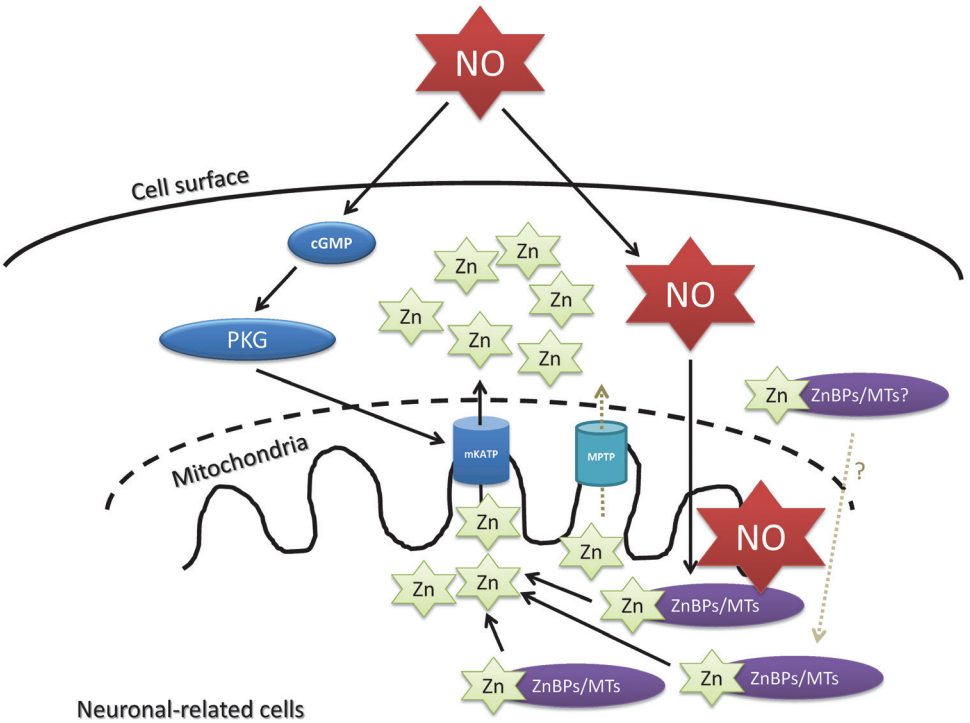

Fig. 7. Working model for the molecular mechanism of live-cell NZR. According to the results of the present study, two downstream pathways from NO are proposed. One is the event directly caused by NO on the mitochondria to induce mitochondrial Zn^{2+} increase. The other is the cGMP/PKG cascade that finally induces the gate opening of mitochondrial ATP-sensitive K^+ channel (mK_{ATP}). Only when the channel activity is initiated can the increased mitochondrial Zn^{2+} be released. Together with the close connections of these two paths, live-cell NZR can be observed. In general, mitochondria play dual roles within NZR. However, MT-1 alone can release Zn^{2+} under the presence of NO donors in living cells and *in vitro*, whereas no clear information about the localization of MTs within mitochondria exists. Thus, certain unknown ZnBPs that may function as the Zn^{2+} pools remain to be identified.

As one of the representative ZnBPs, MT-1 can release Zn^{2+} in the presence of NO *in vitro* (Fig. 3). However, such data are still insufficient to prove that MT-1 is the major ZnBPs for live-cell NZR, especially when considering the dramatic decrease in NRZ caused by PKG and mK_{ATP} blockers (Figs. 2B and 4B). In Kiedrowski's report, the function of the mitochondria was not observed because the study solely manipulated intracellular pH (not NO, even though changing the pH could also be the downstream effect of NO). Given that changing the pH may cause an overall impact on the cells, we did not test the effect of NO on pH or that of pH on cytosolic or mitochondrial Zn^{2+}.

Several studies have reported that Zn^{2+}-bound MT-1 can be imported into the liver mitochondria as the Zn^{2+} pool to regulate respiration.[46] Could this be the source of NZR? From our investigations, we failed to observe any translocation or accumulation of MT-1 into the mitochondria or nucleus during the live-cell NZR (Fig. 6). This observation may be due to several reasons, such as the quality of MT antibodies or other ZnBPs that actually exist in mitochondria (rather than MTs) that are responsible for the NZR Zn^{2+} source. The latter being the real case, the identification of specific mitochondrial ZnBPs for NZR and the knockdown of MT-1 in PC12 cells would be the necessary works in the future.

Basically, from previous reports, NO was proven to generate free zinc through S-nitrosylation reaction. Unless structurally and functionally similar to NO, the mK_{ATP} openers may logically not like NO to efficiently produce free zinc. Therefore, we proposed that the opening of mK_{ATP} and the generation of free zinc could be two independent events. However why diazoxide, the specific mK_{ATP} opener[47–49] still can increase cytosolic zinc (relatively far less amount than NONOate did as shown in Fig. 4D)? We found some clues in previous articles[50,51] which suggest that diazoxide, not like other selective K_{ATP} openers such as pinacidil, favors discrete mitochondrial protein S-Nitrosylation (detail mechanism still remains to be explored). This might provide a proper answer to the above question on Fig. 4D: diazoxide is similar to NO but with less effective ability to generate free zinc.

In conclusion, we propose that the mitochondria perform dual functions in live-cell NZR through a novel molecular mechanism in neuronal-related cells (Fig. 7). The reaction of NO with ZnBPs inside mitochondria is the first event to generate the increase in mitochondrial Zn^{2+}. The later event goes through the cGMP/PKG cascade to open the gate of mitochondrial K_{ATP} channels and to allow increased mitochondrial Zn^{2+} to enter into the intracellular space. Combining both events, the neuronal NZR can be archived. None of these two alone is enough to generate NZR in neuronal cells.

ACKNOWLEDGMENTS

This work was supported by Ministry of Science and Technology of Taiwan, MOST (NSC 102-2320-B-075-002), Taipei Veterans General Hospitals (V106C-194; V107C-008), and Tsou's Foundation (VGHUST102-G7-1-2).

The authors would like to acknowledge Drs. Lung-Sen Kao, Chi-Chang Juan, Hsin-Chen Lee for the suggestions on the article.

REFERENCES

1. Guix FX, Uribesalgo I, Coma M, Muñoz FJ. The physiology and pathophysiology of nitric oxide in the brain. *Prog Neurobiol* 2005;**76**:126–52.

2. Benarroch EE. Nitric oxide: a pleiotropic signal in the nervous system. *Neurology* 2011;**77**:1568–76.
3. Förstermann U, Sessa WC. Nitric oxide synthases: regulation and function. *Eur Heart J* 2012;**33**:829–37, 837a–837d.
4. Moncada S, Bolaños JP. Nitric oxide, cell bioenergetics and neurodegeneration. *J Neurochem* 2006;**97**:1676–89.
5. Calabrese V, Mancuso C, Calvani M, Rizzarelli E, Butterfield DA, Stella AM. Nitric oxide in the central nervous system: neuroprotection versus neurotoxicity. *Nat Rev Neurosci* 2007;**8**:766–75.
6. Wiley JW. The many faces of nitric oxide: cytotoxic, cytoprotective or both. *Neurogastroenterol Motil* 2007;**19**:541–4.
7. Hershfinkel M, Aizenman E, Andrews G, Sekler I. Zinc bells rang in Jerusalem! *Sci Signal* 2010;**3**:mr2.
8. Kelleher SL, McCormick NH, Velasquez V, Lopez V. Zinc in specialized secretory tissues: roles in the pancreas, prostate, and mammary gland. *Adv Nutr* 2011;**2**:101–11.
9. Yamasaki S, Sakata-Sogawa K, Hasegawa A, Suzuki T, Kabu K, Sato E, et al. Zinc is a novel intracellular second messenger. *J Cell Biol* 2007;**177**:637–45.
10. Fukada T, Yamasaki S, Nishida K, Murakami M, Hirano T. Zinc homeostasis and signaling in health and diseases: zinc signaling. *J Biol Inorg Chem* 2011;**16**:1123–34.
11. Pavlica S, Gebhardt R. Comparison of uptake and neuroprotective potential of seven zinc-salts. *Neurochem Int* 2010;**56**:84–93.
12. Bitanihirwe BK, Cunningham MG. Zinc: the brain's dark horse. *Synapse* 2009;**63**:1029–49.
13. Sensi SL, Paoletti P, Bush AI, Sekler I. Zinc in the physiology and pathology of the CNS. *Nat Rev Neurosci* 2009;**10**:780–91.
14. Morris DR, Levenson CW. Ion channels and zinc: mechanisms of neurotoxicity and neurodegeneration. *J Toxicol* 2012;**2012**:785647.
15. Paoletti P, Vergnano AM, Barbour B, Casado M. Zinc at glutamatergic synapses. *Neuroscience* 2009;**158**:126–36.
16. Tóth K. Zinc in neurotransmission. *Annu Rev Nutr* 2011;**31**:139–53.
17. Watt NT, Taylor DR, Kerrigan TL, Griffiths HH, Rushworth JV, Whitehouse IJ, et al. Prion protein facilitates uptake of zinc into neuronal cells. *Nat Commun* 2012;**3**:1134.
18. Kröncke KD, Fehsel K, Schmidt T, Zenke FT, Dasting I, Wesener JR, et al. Nitric oxide destroys zinc-sulfur clusters inducing zinc release from metallothionein and inhibition of the zinc finger-type yeast transcription activator LAC9. *Biochem Biophys Res Commun* 1994;**200**:1105–10.
19. Aravindakumar CT, Ceulemans J, De Ley M. Nitric oxide induces Zn2+ release from metallothionein by destroying zinc-sulphur clusters without concomitant formation of S-nitrosothiol. *Biochem J* 1999;**344 Pt 1**:253–8.
20. Bossy-Wetzel E, Talantova MV, Lee WD, Schölzke MN, Harrop A, Mathews E, et al. Crosstalk between nitric oxide and zinc pathways to neuronal cell death involving mitochondrial dysfunction and p38-activated K+ channels. *Neuron* 2004;**41**:351–65.
21. Lin W, Mohandas B, Fontaine CP, Colvin RA. Release of intracellular Zn(2+) in cultured neurons after brief exposure to low concentrations of exogenous nitric oxide. *Biometals* 2007;**20**:891–901.
22. Jang Y, Wang H, Xi J, Mueller RA, Norfleet EA, Xu Z. NO mobilizes intracellular Zn2+ via cgmp/PKG signaling pathway and prevents mitochondrial oxidant damage in cardiomyocytes. *Cardiovasc Res* 2007;**75**:426–33.
23. Yang DM, Huang CC, Lin HY, Tsai DP, Kao LS, Chi CW, et al. Tracking of secretory vesicles of PC12 cells by total internal reflection fluorescence microscopy. *J Microsc* 2003;**209**(Pt 3):223–7.
24. Chang YF, Teng HC, Cheng SY, Wang CT, Chiou SH, Kao LS, et al. Orai1-STIM1 formed store-operated Ca2+ channels (socs) as the molecular components needed for Pb2+ entry in living cells. *Toxicol Appl Pharmacol* 2008;**227**:430–9.
25. Chiu TY, Teng HC, Huang PC, Kao FJ, Yang DM. Dominant role of Orai1 with STIM1 on the cytosolic entry and cytotoxicity of lead ions. *Toxicol Sci* 2009;**110**:353–62.
26. Chuang TY, Au LC, Wang LC, Ho LT, Yang DM, Juan CC. Potential effect of resistin on the ET-1-increased reactions of blood pressure in rats and Ca2+ signaling in vascular smooth muscle cells. *J Cell Physiol* 2012;**227**:1610–8.
27. Chiu TY, Yang DM. Intracellular Pb2+ content monitoring using a protein-based Pb2+ indicator. *Toxicol Sci* 2012;**126**:436–45.
28. Chiu TY, Chen PH, Chang CL, Yang DM. Live-cell dynamic sensing of Cd(2+) with a FRET-based indicator. *PLoS One* 2013;**8**:e65853.
29. Xi J, Tian W, Zhang L, Jin Y, Xu Z. Morphine prevents the mitochondrial permeability transition pore opening through NO/cgmp/PKG/Zn2+/GSK-3beta signal pathway in cardiomyocytes. *Am J Physiol Heart Circ Physiol* 2010;**298**:H601–7.
30. St Croix CM, Wasserloos KJ, Dineley KE, Reynolds IJ, Levitan ES, Pitt BR. Nitric oxide-induced changes in intracellular zinc homeostasis are mediated by metallothionein/thionein. *Am J Physiol Lung Cell Mol Physiol* 2002;**282**:L185–92.
31. Bernal PJ, Leelavanichkul K, Bauer E, Cao R, Wilson A, Wasserloos KJ, et al. Nitric-oxide-mediated zinc release contributes to hypoxic regulation of pulmonary vascular tone. *Circ Res* 2008;**102**:1575–83.
32. Weissmann N. Nitric-oxide-mediated zinc release: a new (modulatory) pathway in hypoxic pulmonary vasoconstriction. *Circ Res* 2008;**102**:1451–4.
33. Berendji D, Kolb-Bachofen V, Meyer KL, Grapenthin O, Weber H, Wahn V, et al. Nitric oxide mediates intracytoplasmic and intranuclear zinc release. *FEBS Lett* 1997;**405**:37–41.
34. Sensi SL, Ton-That D, Sullivan PG, Jonas EA, Gee KR, Kaczmarek LK, et al. Modulation of mitochondrial function by endogenous Zn2+ pools. *Proc Natl Acad Sci U S A* 2003;**100**:6157–62.
35. Spahl DU, Berendji-Grün D, Suschek CV, Kolb-Bachofen V, Kröncke KD. Regulation of zinc homeostasis by inducible NO synthase-derived NO: nuclear metallothionein translocation and intranuclear Zn2+ release. *Proc Natl Acad Sci U S A* 2003;**100**:13952–7.
36. Potgieter K, Hatcher NG, Gillette R, McCrohan CR. Nitric oxide potentiates camp-gated cation current by intracellular acidification in feeding neurons of pleurobranchaea. *J Neurophysiol* 2010;**104**:742–5.
37. Pravdic D, Vladic N, Cavar I, Bosnjak ZJ. Effect of nitric oxide donors S-nitroso-N-acetyl-DL-penicillamine, spermine nonoate and propylamine propylamine nonoate on intracellular pH in cardiomyocytes. *Clin Exp Pharmacol Physiol* 2012;**39**:772–8.
38. Kiedrowski L. Proton-dependent zinc release from intracellular ligands. *J Neurochem* 2014;**130**:87–96.
39. Carter KP, Young AM, Palmer AE. Fluorescent sensors for measuring metal ions in living systems. *Chem Rev* 2014;**114**:4564–601.
40. Liu Z, Zhang C, Chen Y, He W, Guo Z. An excitation ratiometric Zn2+ sensor with mitochondria-targetability for monitoring of mitochondrial Zn2+ release upon different stimulations. *Chem Commun (Camb)* 2012;**48**:8365–7.
41. Xue L, Li G, Yu C, Jiang H. A ratiometric and targetable fluorescent sensor for quantification of mitochondrial zinc ions. *Chemistry* 2012;**18**:1050–4.
42. Bonanni L, Chachar M, Jover-Mengual T, Li H, Jones A, Yokota H, et al. Zinc-dependent multi-conductance channel activity in mitochondria isolated from ischemic brain. *J Neurosci* 2006;**26**:6851–62.
43. Medvedeva YV, Weiss JH. Intramitochondrial Zn2+ accumulation via the Ca2+ uniporter contributes to acute ischemic neurodegeneration. *Neurobiol Dis* 2014;**68**:137–44.
44. Coetzee WA. Multiplicity of effectors of the cardioprotective agent, diazoxide. *Pharmacol Ther* 2013;**140**:167–75.
45. Pastore D. The puzzle of the molecular identification of mitochondrial potassium channels: progress in animals and impasse in Plants. *Bioenergetics* 2013;**2**:e118.
46. Ye B, Maret W, Vallee BL. Zinc methallothionein imported into liver mitochondria modulates respiration. *Proc Natl Acad Sci U S A* 2001;**98**:2317–22.
47. Cao C, Healey S, Amaral A, Lee-Couture A, Wan S, Kouttab N, et al. ATP-sensitive potassium channel: a novel target for protection against UV-induced human skin cell damage. *J Cell Physiol* 2007;**212**:252–63.
48. Yamada M. Mitochondrial ATP-sensitive K+ channels, protectors of the heart. *J Physiol* 2010;**588**(Pt 2):283–6.
49. Wu H, Wang P, Li Y, Wu M, Lin J, Huang Z. Diazoxide attenuates postresuscitation brain injury in a rat model of asphyxial cardiac arrest by opening mitochondrial ATP-sensitive potassium channels. *Biomed Res Int* 2016;**2016**:1253842.
50. Forbes RA, Steenbergen C, Murphy E. Diazoxide-induced cardioprotection requires signaling through a redox-sensitive mechanism. *Circ Res* 2001;**88**:802–9.
51. Penna C, Perrelli MG, Tullio F, Angotti C, Camporeale A, Poli V, et al. Diazoxide postconditioning induces mitochondrial protein S-nitrosylation and a redox-sensitive mitochondrial phosphorylation/translocation of RISK elements: no role for SAFE. *Basic Res Cardiol* 2013;**108**:371.